

Pitting Corrosion Resistance of Coloured Oxide Films Grown on Stainless Steel in Sulphuric Acid in the Presence and Absence of Chromic Acid

Karina O. Vasconcelos,^a Nerilso Bocchi*^a and Alda M. Simões^b

^aDepartment of Chemistry, Universidade Federal de São Carlos, CP 676, 13560-970 São Carlos-SP, Brazil

^bChemical and Biological Department, Instituto Superior Técnico, Av. Rovisco Pais, 1049-001 Lisboa Codex, Portugal

Neste trabalho foi avaliada a resistência à corrosão por pites de filmes de óxidos coloridos crescidos sobre aço inoxidável AISI 304 em H_2SO_4 e $H_2SO_4 + CrO_3$. A morfologia e topografia dos filmes foram examinadas por MEV (microscopia eletrônica de varredura) e AFM (microscopia de força atômica), respectivamente. As caracterizações eletroquímicas foram conduzidas por curvas de polarização e medidas de impedância em tampão borato pH 9,2. A corrosão por pites foi avaliada por curvas de polarização realizadas na mesma solução contendo NaCl. Todos os filmes coloridos apresentaram valores semelhantes de E_{pit} , mas maiores que dos filmes não coloridos. Os valores de $(E_{pit} - E_{cor})$ resultaram no intervalo de 0,45-0,57 V; 0,78-0,92 V e 0,98-1,12 V para filmes nativos e crescidos na presença e ausência de ácido crômico, respectivamente. Portanto, os filmes crescidos sobre o aço na ausência de ácido crômico apresentaram o maior intervalo de potencial livre de corrosão por pites.

In this work, pitting corrosion resistance of coloured oxides films grown on AISI-304 stainless-steel in H_2SO_4 and $H_2SO_4 + CrO_3$ was evaluated. Surface morphology and topography of the films were examined by SEM (scanning electron microscopy) and AFM (atomic force microscopy), respectively. Electrochemical characterizations were conducted by polarization curves and impedance measurements in borate buffer pH 9.2. The pitting corrosion was evaluated by polarization curves carried out in the same solution containing NaCl. All coloured films presented similar values of E_{pit} , but they were higher than those for non-coloured ones. The values of $(E_{pit} - E_{cor})$ were in the range of 0.45-0.57 V, 0.78-0.92 V and 0.98-1.12 V for native films and films grown in the presence and absence of chromic acid, respectively. Therefore, the films grown on stainless steel in the absence of chromic acid presented the highest potential range free of pitting corrosion.

Keywords: pitting corrosion, coloured oxide films, triangular current scan method, sulphuric acid, sulphuric and chromic acids

Introduction

Coloured stainless steel has introduced a new aesthetic pattern to architecture and decoration since it has good performance in aggressive environments. These coloured oxide films can be grown on the stainless-steel surface by chemical oxidation¹⁻³ or electrochemical oxidation.⁴⁻¹⁰ The chemical process consists of immersion in a hot, concentrated solution of chromic and sulphuric acids and leads to the formation of thick films that seem to result from the dissolution of steel and concomitant reduction of chromic acid.¹ However, chromic-sulphuric acid

solutions are hazardous when used at high temperatures, and therefore the use of electrochemical techniques is a potentially interesting alternative. Ogura *et al.*⁹ proposed to grow films with interference colours by applying either alternating potential pulses⁸ or a triangular current scans to a stainless steel substrate in chromic and sulphuric acid solution at room temperature.

However, it is well known that chromic acid contains Cr^{VI} which is highly toxic.¹¹ Thus far, only two distinct research groups have proposed to carry out the growth of oxide films (colouration) on stainless steel using only sulphuric acid.^{4,12-15} According to the methodology described by Fujimoto *et al.*^{4,12-14} specimens of type 304-stainless steel are immersed in deaerated 0.5 and 5.0 mol L^{-1} H_2SO_4 at 50 °C

*e-mail: bocchi@power.ufscar.br

and immediately submitted to a square-waves polarization for 40 min. In the work of Zhang *et al.*¹⁵ samples of the same steel were coloured in 2.5 mol L⁻¹ H₂SO₄ at 70 °C by applying modulated square-wave potential pulses.

As described above, the two propositions for colouring stainless steels in sulphuric acid employ electrochemical techniques under controlled-potential conditions, but in industrial applications it is much easier to control the current. So, in previous work,¹⁶ the colouration of stainless steel was investigated only in 5 mol L⁻¹ H₂SO₄ at different temperatures by applying triangular current scans. Thickest oxide films were formed on stainless steel samples in 5 mol L⁻¹ H₂SO₄, kept at 50 °C, using the following experimental parameters: $i_{\min} = -0.81 \text{ mA cm}^{-2}$, $i_{\max} = 1.40 \text{ mA cm}^{-2}$ and $\tau = 2.5 \text{ s}$. The electrolysis of the steel samples carried out in these experimental conditions lead to oxide films whose thicknesses increased (<100-280 nm) with the electrolysis time (20-60 min). The predominant colours were gold, red and blue, although intermediate colours (greenish yellow, greenish blue and brown) were also observed, depending on the electrolysis time.

There seems to be an agreement that the corrosion resistance is increased for coloured oxide films formed on stainless steel using sulphuric acid in the presence of chromic acid. Wang *et al.*^{17,18} characterized the pitting corrosion of coloured samples obtained by chemical, INCO (chemical colouring + electrolytic hardening) and electrochemical (square-wave potential pulses) processes, using anodic polarization and electrochemical impedance spectroscopy in a HCl solution. Their experimental results showed that the pitting resistance of the coloured samples increased in the following process order: chemical < electrochemical < INCO. In previous work,¹⁹ it was evaluated the resistance to uniform and pitting corrosion of AISI-304 stainless-steel samples coloured by alternating potential pulses with different amplitudes and electrolysis times. All the different coloured samples were less susceptible to uniform corrosion than the non-coloured ones. A comparative study of the resistance to pitting corrosion for differently coloured AISI-304 stainless-steel samples (chemical and electrochemical methods) was also reported previously.²⁰ It was concluded that coloured oxide films have a protective effect against pitting corrosion independently of the colouring methods under accelerated test in deaerated 0.62 mol L⁻¹ NaCl solution and for the first hours of extended immersion tests in 0.40 mol L⁻¹ HCl solution, when compared with non-coloured film. For longer exposition times (8-10 h) the non-coloured and coloured steel samples present the same behaviour.

On the other hand, for steel samples coloured in the absence of chromic acid, Fujimoto *et al.*¹² have reported

that films formed in this condition never inhibited any initiation of localised corrosion in chloride solution. From TEM (transmission electron microscopy) micrographs, these authors have concluded that the film seems to contain many pathways, which permit subsequent growth without any decrease in the rate and penetration of water and/or ions.

As highlighted hereinbefore, the colouring methods constitute an effective way of increasing the corrosion resistance and applications of stainless steel. Moreover, as far as we know there are no studies on the pitting corrosion resistance of stainless steels coloured using only sulphuric acid and the triangular current scan method. Thus, in the present work a comparative study of the pitting corrosion resistance of coloured oxides films grown by triangular current scan method in sulphuric acid with and without chromium acid is reported.

Experimental

Material and electrochemical colouring

A 150 mL conventional three-electrode electrochemical cell was used for colouring the stainless-steel samples, which were the working electrodes. Two spiral Pt wires were used as auxiliary electrodes, and an Hg/Hg₂SO₄ electrode in a 5.0 mol L⁻¹ H₂SO₄ solution as reference. Stainless-steel samples 2 × 5 cm in size were cut from a sheet (0.5 mm thick) of bright annealed austenitic AISI-304 stainless steel (ACESITA # 2B) with the following mass composition: Cr 17.7%, Ni 7.4%, Mn 1.2%, Si 0.4%, S 0.01%, C 0.07%, and Fe balanced.

The stainless-steel samples were firstly degreased for 10 min with acetone under ultrasonic stirring and then rinsed in distilled water. After being electroreduced ($i = -1.0 \text{ mA cm}^{-2}$) for 20 min in an aqueous 1.0 mol L⁻¹ HNO₃ solution,⁹ the pre-treated steel samples were then immersed in an aqueous 5.0 mol L⁻¹ H₂SO₄ solution with and without 2.5 mol L⁻¹ CrO₃ and immediately submitted to a triangular current scan pre-programmed in the GPES software used to control an Autolab PGSTAT30 potentiostat/galvanostat from Eco Chemie. After colouring, the stainless-steel samples were removed from the solution, rinsed thoroughly with distilled water and dried in air.

The experimental parameters of the triangular current scan method used for colouring the steel samples in 5.0 mol L⁻¹ H₂SO₄ solution with 2.5 mol L⁻¹ CrO₃ were the same those employed by Ogura *et al.*⁹ The current density values varied from $i_{\min} = -0.81 \text{ mA cm}^{-2}$ to $i_{\max} = 2 \text{ mA cm}^{-2}$. Electrolyses were carried out at 25 °C for 50 min, where films of thickness of approximately 260 nm were formed.

For electrolyses carried out in an aqueous 5.0 mol L⁻¹ H₂SO₄ solution only, the experimental parameters of the triangular current scan method were chosen following the results previously reported by Vasconcelos *et al.*¹⁶ The current density values varied from $i_{\min} = -0.81$ mA cm⁻² to $i_{\max} = 1.4$ mA cm⁻² at 50 °C. In order to obtain films with comparable thickness with those grown in the presence of chromic acid, a time of electrolysis of 60 min were used. Films of thickness near of 240 nm were obtained in this case.

Characterisation of the films

The thickness of the coloured oxide films grown on the stainless-steel samples were estimated by measuring their spectral reflectance in the visible region (400-700 nm) using a spectra Gretag Macbeth-2180 spectrophotometer.

The surface morphology of the coloured oxide films grown by triangular current scan method in sulphuric acid with and without chromium acid was examined by scanning electron microscopy (SEM). The apparatus was the Digital Instruments IIIA. AFM images of these same films were also obtained using a Nanoscope system, operating in contact mode with a silicon tip.

Electrochemical measurements

The electrochemical studies, in order to evaluate the protective effect of the oxide films grown on the stainless-steel samples against pitting corrosion, were conducted at room temperature by potentiodynamic polarization curves. For such, a conventional electrochemical cell with three electrodes was used. The counter electrode was a Pt-spiral and a saturated calomel electrode (SCE) was used as reference for the potential measurements. A Gamry FAS1 Femtostat potentiostat controlled by the software EIS 300 was used to obtain the polarization curves. In order to eliminate edge effects, epoxy resin was applied in all coloured samples; only one of the faces (square area of 1 cm²) was not covered. The coloured samples were immersed in an aqueous borate buffer solution of pH 9.2 [0.050 mol L⁻¹ H₃BO₃ (Merck p.a.) + 0.075 mol L⁻¹ Na₂B₄O₇·10H₂O (Riedel-de Haen analytical reagent)] without and with 0.7 mol L⁻¹ NaCl (Panreac), at room temperature, and kept at the open circuit potential. After the corrosion potential was practically stable (*ca.* 40 min), the steel sample was polarized to more negative of *ca.* 30 mV than the corrosion potential. The potentiodynamic polarization curve was then immediately initiated in the anodic direction (up to *ca.* 1.1 V *vs.* SCE) at a sweep rate of 1 mV s⁻¹. At least three polarization curves were always obtained for each one of the steel samples electrolysed in a

given experimental condition. The results were normalized to the geometrical area of the samples.

EIS (electrochemical impedance spectroscopy) measurements were also conducted for the coloured-steel samples in borate buffer solution pH 9.2 containing 0.7 mol L⁻¹ NaCl. These measurements were obtained at the open circuit potential, applying a 10 mV (rms) ac signal and scanning the 100 kHz-10 mHz frequency range. The analysis was performed in Gamry FAS1 Femtostat potentiostat controlled by the software EIS 300. The results were also normalized to the samples geometrical area.

Results and Discussion

Typical potentiodynamic polarization curves, obtained in borate buffer pH 9.2 for steel samples in the three situations investigated (as received and coloured in the presence and absence of chromic acid), are shown in Figure 1. Comparing two of these curves (a and c) with those previously reported,²¹ two main differences are observed for potentials lower than 0.6 V *vs.* ECS. The curves in Figure 1 present lower values of current density and higher values of corrosion potential. This possibly occurs because the edge effects were eliminated by applying epoxy resin in the steel samples. Therefore, the oxide films (native and grown on steel samples) are more protective in the present work. Among the curves in Figure 1, the values of current density are higher for coloured than non-coloured samples for the same overpotential in the passive region (see values of $-\log i$ for $\eta = 0.2$ V in the figure). The increases in the values of current density are close to one and two order of magnitude for steel samples coloured in H₂SO₄ and H₂SO₄

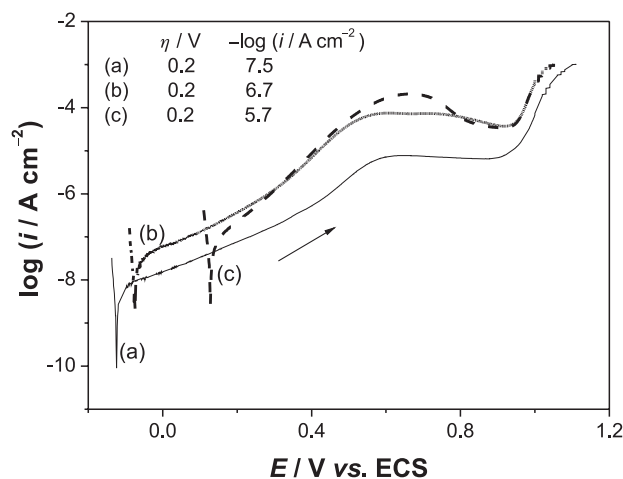


Figure 1. Typical potentiodynamic polarization curves ($v = 1$ mV s⁻¹) obtained at room temperature in a borate buffer solution pH 9.2 for AISI-304 stainless-steel (a) non-coloured sample (as received) and previously coloured samples using the triangular current scans method in (b) 5.0 mol L⁻¹ H₂SO₄ and (c) 5.0 mol L⁻¹ H₂SO₄ + 2.5 mol L⁻¹ CrO₃.

+ CrO_3 , respectively. These results indicate that oxide films with distinct surface areas were grown on the steel surface. So, the oxide films grown in $\text{H}_2\text{SO}_4 + \text{CrO}_3$ have more surface area than those grown in only H_2SO_4 . Figure 2 shows typical micrographs obtained for steel samples in the three situations investigated (as received and coloured in the presence and absence of chromic acid). A compact and uniform oxide film is spontaneously formed on steel surface (Figure 2a). On the other hand, highly porous

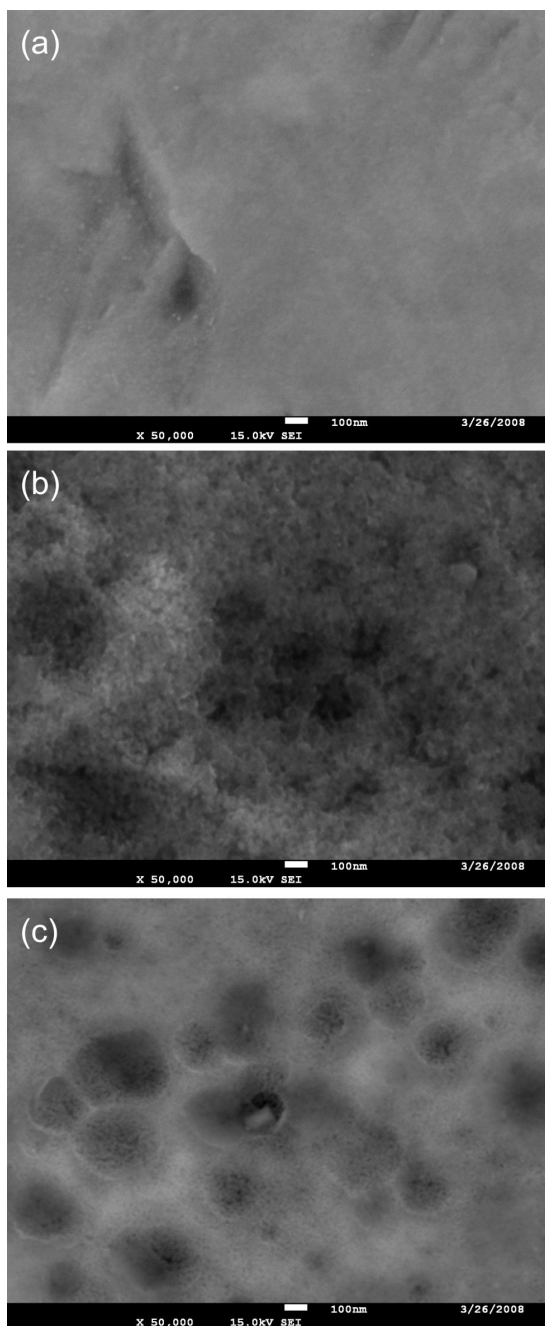


Figure 2. Typical micrographs obtained by SEM for AISI-304 stainless-steel (a) non-coloured (as received) and previously coloured samples using the triangular current scans method in (b) $5.0 \text{ mol L}^{-1} \text{H}_2\text{SO}_4$ and (c) $5.0 \text{ mol L}^{-1} \text{H}_2\text{SO}_4 + 2.5 \text{ mol L}^{-1} \text{CrO}_3$.

films are grown on steel by the triangular current scan method (Figures 2b and c). However, these figures do not distinguish differences in porosity between oxide films grown in H_2SO_4 with and without CrO_3 . Kikuti *et al.*²¹ have also observed by SEM the growth of highly porous oxide films in $\text{H}_2\text{SO}_4 + \text{CrO}_3$ when the triangular current scan method was employed. Figure 3 presents typical surface topographies obtained for steel samples in the three

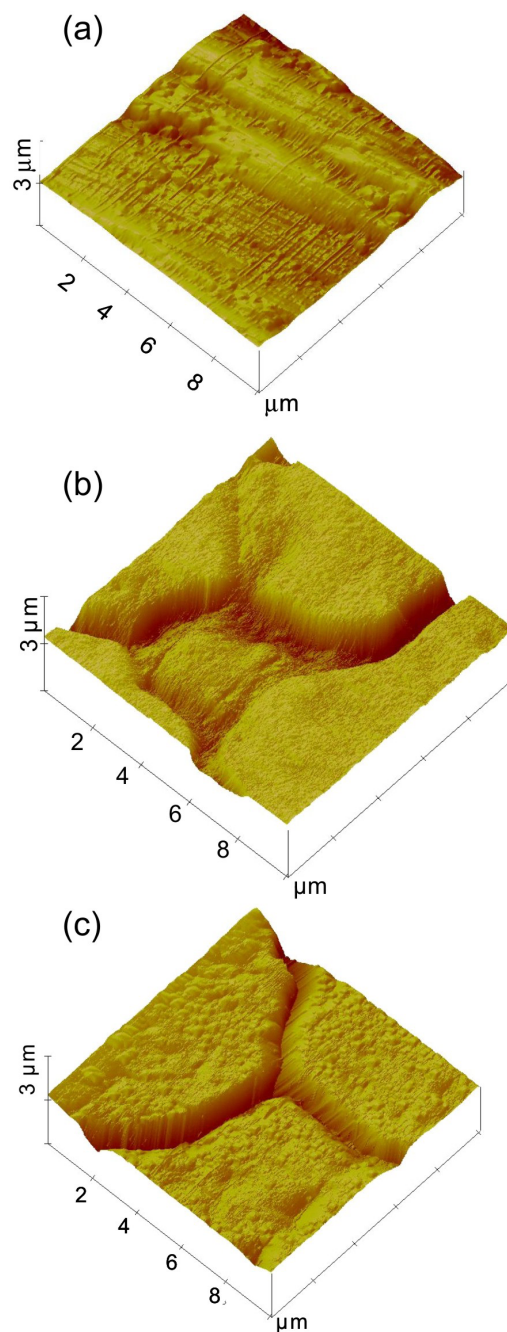


Figure 3. Typical surface topographies obtained by AFM for AISI-304 stainless-steel (a) non-coloured (as received) and previously coloured samples using the triangular current scans method in (b) $5.0 \text{ mol L}^{-1} \text{H}_2\text{SO}_4$ and (c) $5.0 \text{ mol L}^{-1} \text{H}_2\text{SO}_4 + 2.5 \text{ mol L}^{-1} \text{CrO}_3$.

situations investigated (as received and coloured in the presence and absence of chromic acid). From roughness analysis in various AFM images of different sizes ($100\ \mu\text{m}^2$, $2,500\ \mu\text{m}^2$ and $10,000\ \mu\text{m}^2$) the films grown either in H_2SO_4 or $\text{H}_2\text{SO}_4 + \text{CrO}_3$ reveal surface areas 6-20% higher than AFM image areas; whereas oxide films spontaneously formed on steel present surface areas of 3-5% higher than AFM image areas. Therefore, only differences in porosity may explain why oxide films grown in $\text{H}_2\text{SO}_4 + \text{CrO}_3$ have more surface area than those grown in only H_2SO_4 as observed by polarization curves (Figure 1).

The pitting corrosion susceptibility of the oxide films formed on the stainless-steel samples in the three situations (as received and grown in the presence and absence of chromic acid) was evaluated by potentiodynamic polarization curves carried out in a borate buffer solution pH 9.2, containing chloride ions (Figure 4). After these measurements, the visual colour of all steel samples was practically unchanged. As already pointed out in Figure 1, the values of current density are also higher for coloured (near one order of magnitude) than non-coloured samples for the same overpotential in the passive region. The values of E_{cor} , E_{pit} and $(E_{\text{pit}} - E_{\text{cor}})$ extracted from the potentiodynamic polarization curves of Figure 4 for steel samples non-coloured and previously coloured using the triangular current scan method are listed in Table 1. All coloured steel samples present similar values of E_{pit} but they are higher than those for non-coloured ones. By the other hand, the values of $(E_{\text{pit}} - E_{\text{cor}})$ are in the range of 0.45 V-0.57 V, 0.78 V-0.92 V and 0.98 V-1.12 V for native films (very thin films) and films grown (thicker films) in the presence and absence of chromic acid, respectively. These

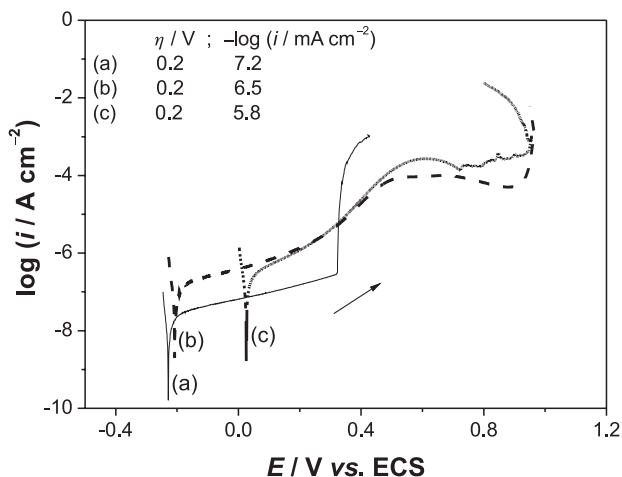


Figure 4. Typical potentiodynamic polarization curves ($\nu = 1\ \text{mV s}^{-1}$) obtained at room temperature in a borate buffer solution pH 9.2 containing $0.7\ \text{mol L}^{-1}$ NaCl for AISI-304 stainless-steel (a) non-coloured sample (as received) and previously coloured samples using the triangular current scans method in (b) $5.0\ \text{mol L}^{-1}$ H_2SO_4 and (c) $5.0\ \text{mol L}^{-1}$ $\text{H}_2\text{SO}_4 + 2.5\ \text{mol L}^{-1}$ CrO_3 .

results show that the films grow on stainless steel in the absence of chromic acid present the highest potential range free of pitting corrosion. So, the films grown on stainless steel in this condition are more protective against pitting corrosion. A possible explanation for these results can be given assuming that the porous of coloured films are of the isolated type, *i.e.* the porous begin in the top of the films but do not reach the steel substrat.²² Moreover, oxide films with lower porous density may also possibly explain the results for films grown in H_2SO_4 , as they represent a greater physical barrier. Less porosity leads to less free pathways for penetration of water and ions and so, less pitting corrosion susceptibility.

Table 1. Values of E_{cor} , E_{pit} and $(E_{\text{pit}} - E_{\text{cor}})$ from potentiodynamic polarization curves obtained in borate buffer solution pH 9.2 + $0.7\ \text{mol L}^{-1}$ NaCl for AISI-304 stainless-steel non-coloured and previously coloured samples using the triangular current scan method

	$E_{\text{cor}} / \text{V}$	$E_{\text{pit}} / \text{V}$	$(E_{\text{pit}} - E_{\text{cor}}) / \text{V}$
Native films	-0.217	0.326	0.543
	-0.228	0.223	0.451
	-0.205	0.368	0.573
Films grown in H_2SO_4	-0.184	0.935	1.119
	-0.200	0.779	0.979
	-0.206	0.907	1.113
Films grown in $\text{H}_2\text{SO}_4 + \text{CrO}_3$	0.024	0.949	0.925
	0.048	0.941	0.893
	0.052	0.830	0.778

As shown in Figure 5, impedance spectra were also obtained at the open circuit potential in borate buffer pH 9.2 containing $0.7\ \text{mol L}^{-1}$ NaCl for steel samples in the three situations investigated (as received and coloured in the presence and absence of chromic acid). It is important to mention that these impedance spectra are similar those obtained at the same buffer solution in the absence of chloride ions.²¹ As previously reported, the impedance response of the films was also capacitive for most of the spectrum.

Like in a previous work,²¹ the fitting of capacitive part of the spectra was also made using a constant phase element (CPE), whose impedance is given by:

$$Z_{\text{CPE}} = \frac{1}{Y_0(j\omega)^n}$$

where ω is the angular frequency, Y_0 the frequency-independent parameter, n related to the phase angle and gives information on the type of element ($n = 1$ for a capacitor and $n = 0$ for a resistor) and $j = (-1)^{1/2}$. For native films and films grown in the presence and absence of chromic acid, the equivalent circuit (EC) as well as the results of the fitting is presented in Figure 5 and Table 2. The values of Y_0 were

practically the same for native film and film grown in H_2SO_4 . Unlikely, the value of Y_0 for the film grown in $\text{H}_2\text{SO}_4 + \text{CrO}_3$ was more than one order of magnitude higher than those of

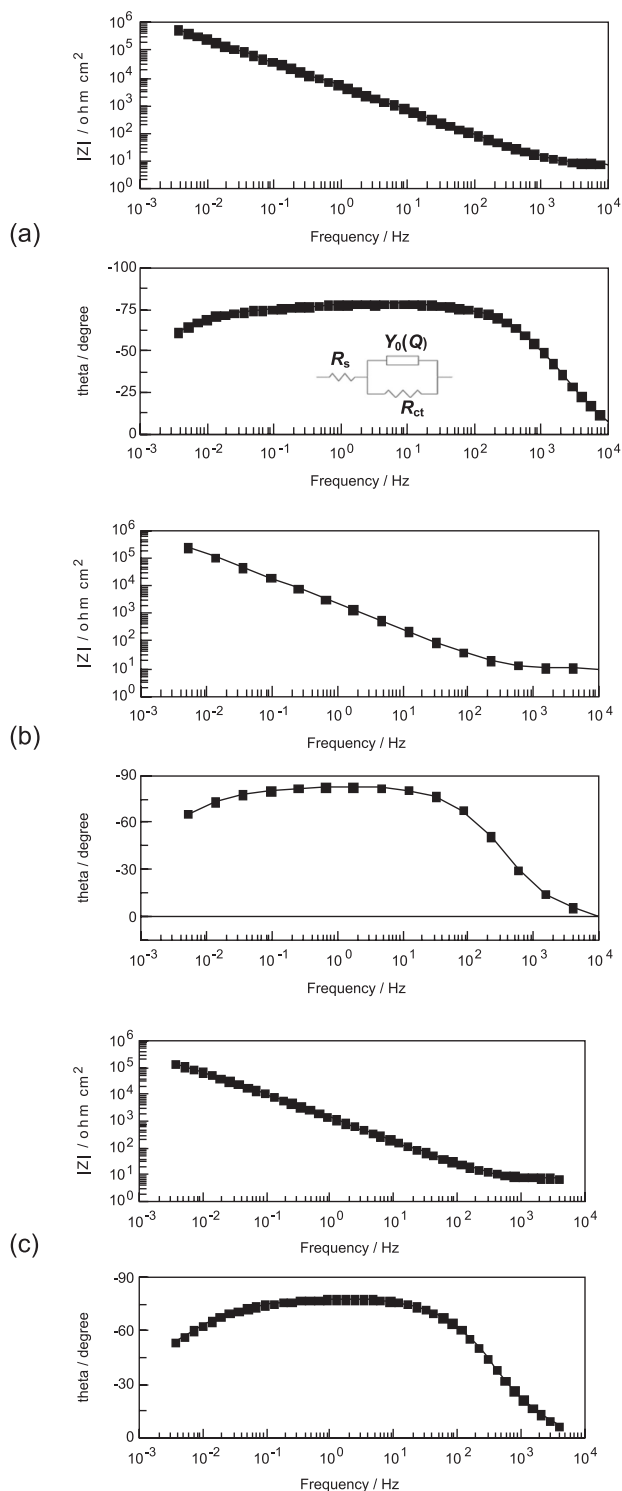


Figure 5. Impedance spectra obtained at the open circuit potential and room temperature in a borate buffer solution pH 9.2 containing 0.7 mol L^{-1} NaCl for AISI-304 stainless-steel (a) non-coloured sample (as received) and previously coloured samples using the triangular current scans method in (b) $5.0 \text{ mol L}^{-1} \text{H}_2\text{SO}_4$ and (c) $5.0 \text{ mol L}^{-1} \text{H}_2\text{SO}_4 + 2.5 \text{ mol L}^{-1} \text{CrO}_3$.

Table 2. Values used in the fitting of EIE spectra

	$Y_0(Q) /$ ($\text{F cm}^{-2} \text{s}^{-n}$)	n	$R_{ct} /$ ($\Omega \text{ cm}^2$)	X^2
Native films	4.0×10^{-5}	0.87	1.6×10^6	2.1×10^{-3}
Films grown in H_2SO_4	8.4×10^{-5}	0.92	7.5×10^5	2.2×10^{-3}
Films grown in $\text{H}_2\text{SO}_4 + \text{CrO}_3$	1.5×10^{-4}	0.86	2.7×10^5	1.8×10^{-3}

the other films. Since there was no change in the equivalent circuit of the spectrum and the value of Y_0 is proportional to the area, this increase suggests that the area contributing to the values of Y_0 has increased. The area increase can be explained by an increased surface area in the film, *i.e.*, by the thickness of a more porous film, as suggested hereinbefore. The fact that there is only one time constant in the spectrum also suggests identical properties for the walls and the bottom of the pores.

R_{ct} accounts for the charge transfer resistance at the film surface. Its estimate is affected by a relatively high error since its response comes mostly below the low frequency of the spectrum. In spite of this, the fact that it decreases for films grown in $\text{H}_2\text{SO}_4 + \text{CrO}_3$ is in agreement with the development of an extended area. These results indicate that the porosity of the films grown on stainless steel by the triangular current scan method increases with CrO_3 addition, which corroborates the interpretation given for the obtained results of pitting corrosion.

Conclusions

Thick passive films showing interference colours have been grown on stainless steel in aqueous solution of $5.0 \text{ mol L}^{-1} \text{H}_2\text{SO}_4$ and $5.0 \text{ mol L}^{-1} \text{H}_2\text{SO}_4 + 2.5 \text{ mol L}^{-1} \text{CrO}_3$ by the triangular current scan method. Films of thickness near of 240 nm and 260 nm were formed in H_2SO_4 (at 50°C) and $\text{H}_2\text{SO}_4 + \text{CrO}_3$ (at 25°C), respectively. All coloured films presented similar values of E_{pit} but they were higher than those for non-coloured ones. The values of $(E_{\text{pit}} - E_{\text{cor}})$ were in the range of 0.45-0.57 V, 0.78-0.92 V and 0.98-1.12 V for native films and films grown in the presence and absence of chromic acid, respectively. Therefore, the films grown on stainless steel in the absence of chromic acid presented the highest potential range free of pitting corrosion. This was explained by a film formation with lower number of porous as suggested by impedance measurements.

Acknowledgements

The authors gratefully acknowledge the Brazilian research funding agencies FAPESP, CNPq and CAPES for

the financial support of this work. The authors also thank Prof. Dr. Rodrigo del Rio from Pontificia Universidad Católica de Chile for the AFM images.

References

1. Evans, T. E.; Hart, A. C.; James, H.; Smith, V. A.; *Trans. Inst. Met. Finish.* **1972**, *51*, 108.
2. Evans, T. E.; *Corros. Sci.* **1977**, *17*, 105.
3. Evans, T. E.; Hart, A. C.; Skedgell, A. E.; *Trans. Inst. Met. Finish.* **1973**, *50*, 77.
4. Fujimoto, S.; Shibata, T.; Wada, K.; Tsutae, T.; *Corros. Sci.* **1993**, *35*, 147.
5. Lin, C. J.; Duh, J. G.; *Surf. Coat. Technol.* **1994**, *70*, 79.
6. Lin, C. J.; Duh, J. G.; *Surf. Coat. Technol.* **1995**, *73*, 52.
7. Lin, C. J.; Duh, J. G.; *Surf. Coat. Technol.* **1996**, *85*, 175.
8. Ogura, K.; Sakurai, K.; Uehara, S.; *J. Electrochem. Soc.* **1994**, *141*, 648.
9. Ogura, K.; Lou, W.; Nakayama, M.; *Electrochim. Acta* **1996**, *41*, 2849.
10. Ogura, K.; Tsujigo, M.; Sakurai, K.; Yano, J.; *J. Electrochem. Soc.* **1993**, *140*, 1311.
11. Rajeshwar, K.; Ibanez, J. G.; *Environmental Electrochemistry*, Academic Press: San Diego, 1997.
12. Fujimoto, S.; Shibata, T.; *Mater. Sci. Forum* **1995**, *185*, 741.
13. Fujimoto, S.; Kiyoshi, T.; Shibata, T.; *J. Electroanal. Chem.* **1999**, *473*, 265.
14. Fujimoto, S.; Kawachi, S.; Nishio, T.; Shibata, T.; *Electrochim. Acta* **2001**, *47*, 543.
15. Zhang, J. X.; Chen, J.; Qiao, Y. N.; Cao, C. N.; *Trans. Inst. Met. Finish.* **1999**, *77*, 106.
16. Vasconcelos, K. O.; Bocchi, N.; Rocha, R. C.; Biaggio, S. R.; *J. Electrochem. Soc.* **2005**, *152*, B491.
17. Wang, J. H.; Duh, J. G.; Shih, H. C.; *J. Mater. Sci. Lett.* **1995**, *14*, 53.
18. Wang, J. H.; Duh, J. G.; Shih, H. C.; *Surf. Coat. Technol.* **1996**, *78*, 248.
19. Conrado, R.; Bocchi, N.; Rocha-Filho, R. C.; Biaggio, S. R.; *Electrochim. Acta* **2003**, *48*, 2417.
20. Kikuti, E.; Conrado, R.; Bocchi, N.; Biaggio, S. R.; Rocha-Filho, R. C.; *Electrochim. Acta* **2004**, *15*, 472.
21. Kikuti, E.; Bocchi, N.; Pastol, J. L.; Ferreira, M. G.; Montemor, M. F.; Da Cunha Belo, M.; Simões, A. M.; *Corr. Sci.* **2007**, *49*, 2303.
22. Kutzelnigg, A.; *Plating* **1961**, *48*, 382.

Received: April 30, 2009

Web Release Date: December 3, 2009

FAPESP helped in meeting the publication costs of this article.